

# DNA Origami-Enabled Engineering of Ligand–Drug Conjugates for Targeted Drug Delivery

Zhilei Ge, Linjie Guo, Guangqi Wu, Jiang Li, Yunlong Sun, Yingqin Hou, Jiye Shi, Shiping Song, Lihua Wang, Chunhai Fan, Hua Lu,\* and Qian Li\*

Effective drug delivery systems that can systematically and selectively transport payloads to disease cells remain a challenge. Here, a targeting ligand-modified DNA origami nanostructure (DON) as an antibody–drug conjugate (ADC)-like carrier for targeted prostate cancer therapy is reported. Specifically, DON of six helical bundles is modified with a ligand 2-[3-(1,3-dicarboxy propyl)-ureido] pentanedioic acid (DUPA) against prostate-specific membrane antigen (PSMA), to serve as the antibody for drug conjugation in ADC. Doxorubicin (Dox) is then loaded to DON through intercalation to dsDNA. This platform features in spatially controllable organization of targeting ligands and high drug loading capacity. With this nanocomposite, selective delivery of Dox to the PSMA+ cancer cell line LNCaP is readily achieved. The consequent therapeutic efficacy is critically dependent on the numbers of targeting ligand assembled on DON. This target-specific and biocompatible drug delivery platform with high maximum tolerated doses shows immense potential for developing novel nanomedicine.

under the context that Brentuximab vedotin (Adcetris) for relapsed Hodgkin lymphoma<sup>[5,6]</sup> and T-DM1 (Kadcyla) for HER2<sup>+</sup> metastatic breast cancer<sup>[7,8]</sup> received clinical approval from the Food and Drug Administration (FDA). The so-called “magic bullet,” originally conceived by Paul Ehrlich,<sup>[9]</sup> are designed to combine the toxicity of small-molecule drugs with the targeting ability of antibodies to improve overall efficacy and therapeutic index.<sup>[10–15]</sup> Although conceptually straightforward, development of ADCs is encountered with several challenges including manageable toxicity, homogeneous conjugation and limited drug payload capacity. The balance between drug-to-antibody ratio (DAR) and targeting capability is mandatory for ADCs to reduce the attrition rate of drug candidates. Very high

## 1. Introduction

Antibody drug conjugates (ADCs) have emerged as powerful anticancer therapeutics in the past decade,<sup>[1–4]</sup> especially

DAR ADCs may suffer decreased recognition to the target antigen.<sup>[16–19]</sup> Hence, it is highly desirable to develop ADCs with both high maximum tolerated doses and high selectivity.<sup>[20–22]</sup>


Prof. Z. Ge, Prof. C. Fan, Prof. Q. Li  
 School of Chemistry and Chemical Engineering  
 and Institute of Molecular Medicine  
 Renji Hospital  
 School of Medicine  
 Shanghai Jiao Tong University  
 Shanghai 200240, China  
 E-mail: liqian2018@sjtu.edu.cn

Recently, the bloom of structural DNA nanotechnology<sup>[23,24]</sup> has demonstrated unprecedented precision on structural control, which enables predictable and programmable construction of complex nanostructures by exploiting intra- and inter-molecular Watson-Crick base-pairing. The programmability and addressability of DNA origami nanostructures (DONs) enable multiple desired functional moieties (such as therapeutic cargoes and tumor targeting ligands) with designer geometry and density.<sup>[25–27]</sup> Therefore, DONs have been increasingly employed for developing novel drug delivery systems<sup>[28,29]</sup> due to their versatile designability, high solubility, and intrinsic biocompatibility.<sup>[30–37]</sup> Moreover, certain types of DONs have been proven to be readily rapidly internalized by mammalian cells despite their negatively charged surface property.<sup>[38]</sup>

L. Guo, Prof. J. Li, Dr. J. Shi, Prof. S. Song, Prof. L. Wang  
 Division of Physical Biology & Bioimaging Center  
 Shanghai Synchrotron Radiation Facility  
 Shanghai Institute of Applied Physics  
 Chinese Academy of Sciences  
 Shanghai 201800, China

G. Wu, Y. Sun, Y. Hou, Prof. H. Lu  
 Beijing National Laboratory for Molecular Sciences  
 Center for Soft Matter Science and Engineering  
 Key Laboratory of Polymer Chemistry and Physics  
 of Ministry of Education  
 College of Chemistry and Molecular Engineering  
 Peking University  
 Beijing 100871, China  
 E-mail: chemhualu@pku.edu.cn

We herein propose that DONs with certain framework<sup>[39]</sup> could serve as an ideal scaffold for ADCs analogues with exceptional control over targeting ligand density and drug loading contents for optimized antitumor efficacies and safety profile.<sup>[40]</sup> Specifically, we construct a new prostate cancer (PCa)-specific drug delivery system by introducing different numbers of ligand 2-[3-(1,3-dicarboxy propyl)-ureido] pentanedioic acid (DUPA) to a designed six-helical-bundle DNA origami nanostructure (6HB DON). DUPA has been demonstrated to be a high-affinity inhibitor ( $K_i \approx 0.02 \times 10^{-9} - 0.1 \times 10^{-9}$  M) for prostate-specific membrane antigen (PSMA).<sup>[41]</sup> We incorporate this

 The ORCID identification number(s) for the author(s) of this article can be found under <https://doi.org/10.1002/sml.201904857>.

DOI: 10.1002/sml.201904857

ligand through DNA hybridization of DUPA modified single strand DNA (ssDNA) with DONs to form a DNA based “antibody” targeting PSMA<sup>+</sup> prostate cancer cells. The site-specificity of DONs allows us to manage a controllable and programmable distribution of DUPA ligand on DONs. The chemotherapeutic drug doxorubicin (Dox) can be easily loaded to these nanocarriers via intercalation to double strand DNA (dsDNA), forming ADC-like nanocomposites with high drug loading capacity. The therapeutic efficacy of thus fabricated nanocomposites is highly dependent on the distribution of targeting ligand DUPA on DONs, demonstrating a better capability for potential treatment efficacy.

## 2. Results and Discussion

### 2.1. Design, Construction, and Characterization of ADC-Like Nanocomposites

One particular advantage of DONs over traditional ADCs is that they can provide two orders of magnitude higher drug payload capacity. In addition, multiple binding sites of DONs allow for the loading of both the nanodrugs and targeting ligands by either chemical modification or physical association.<sup>[42]</sup> A 3D tubular DON composed of six helical bundles (6HB) was designed to serve as the drug carrier selectively against target cells (Figure 1a,b). Long linear topology of 6HB could offer higher drug payload capacity, cellular uptake efficiency<sup>[32]</sup> and prolonged circulation of half-lives in vivo.<sup>[43]</sup> Briefly, the 6HB-DON was constructed from a 7249-nucleotide-long M13 bacteriophage

genome DNA and multiple short-single strands, following a single-step annealing process<sup>[44,45]</sup> Thus prepared DON carriers were further characterized by agarose gel electrophoresis, atomic force microscopy (AFM) and transmission electron microscopy (TEM). Based on the size parameters of B-form double-helix DNA (2 nm diameter, and 0.33 nm per base in the direction of the helical axis), this 6HB DON was 400 nm in length with cross-section of 6 nm by 6 nm. Discrete bands with expected mobility were observed in native agarose gel electrophoresis analysis, that a slightly decreased mobility for the DON is observed compared to the single-stranded M13 DNA, suggesting the formation of designed origami structures (Figure S5a, Supporting Information, Lane 2). The corresponding bands of DONs were then extracted from the gel for imaging characterization by AFM and TEM (Figure 1a), which unambiguously confirmed the formation of DONs with expected size and shape.

DUPA-DNA conjugate (sequence: 5'-DUPA-TTGGTGGTG-GTGGTGGTGGT-3') was synthesized and verified by electrospray ionization mass spectrometry (Figures S1–S4, Supporting Information), and then intentionally introduced into tubular DONs via hybridization with unpaired DNA single strand (sequence: 5'-ACCACCACCACCACCACC-3'). Specifically, the DUPA binding sites on 6HB-DONs were rationally designed (Figure S6, Supporting Information). Four different DON carriers with 5, 10, 20, and 30 binding sites on each DON were designated, with a corresponding inter-distance of 240 nt (80 nm), 120 nt (40 nm), 60 nt (20 nm), and 40 nt (13.3 nm) between neighboring DUPA ligands, respectively.

Due to its preferential intercalation into double-stranded 5'-GC-3' or 5'-CG-3', Dox was loaded to DONs by simply

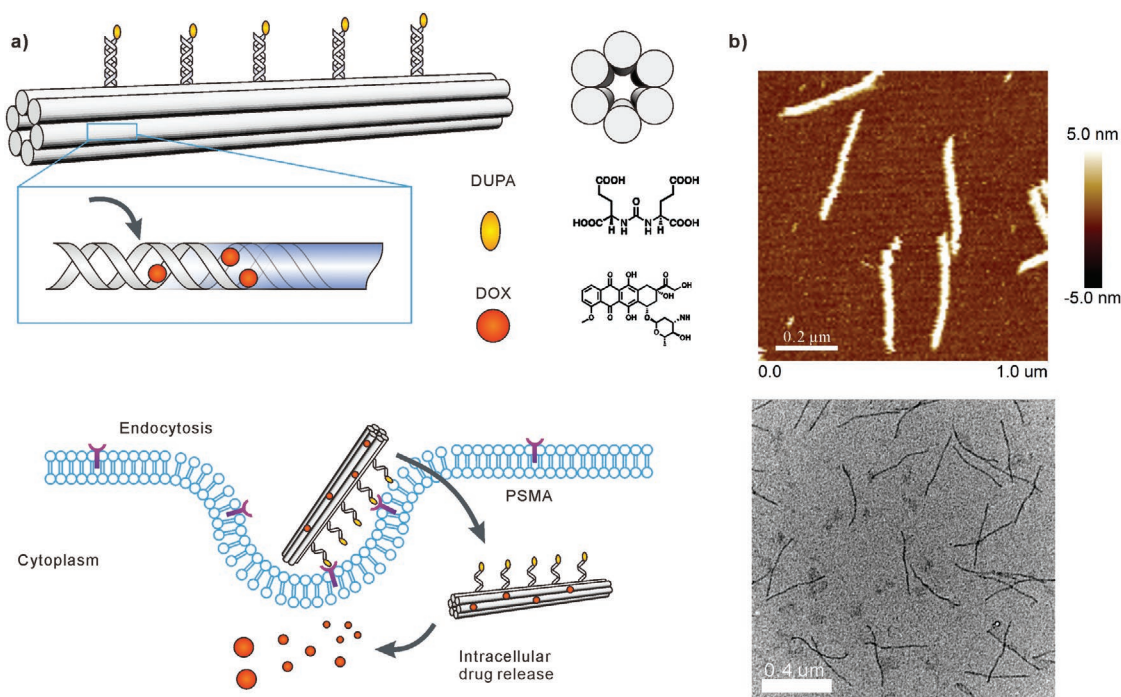


**Figure 1.** Six-helical-bundle DNA origami nanostructure (6HB-DONs) as drug carriers. a) Schematic illustration of the ADC-like nanocomposites and its working principle. b) Representative AFM image (top panel) and TEM image (bottom panel) of 6HB-DONs. Scale bars, 0.2 μm in AFM image and 0.4 μm in TEM image.

incubating DONs with free Dox at 25 °C in 1× TAE/Mg<sup>2+</sup> buffer. The UV spectra of Dox and Dox-loaded DONs were shown in Figures S7 and S8 in the Supporting Information. Based on the absorbance at 260 nm (corresponding to DNA) and 480 nm (corresponding to DOX) in the UV spectra, the average stoichiometric ratio between DON and Dox molecules was calculated to be 1:3200 (Figure S7, Supporting Information). Whereas for antibody-directed ADC, the chemical profile generally offers not more than eight conjugation sites for drugs. This high drug payload capacity of DONs could substantially increase the therapeutic index and optimize the loading contents for antitumor efficacies and safety profile.

Pristine DONs, Dox-DONs, and Dox-DUPA-DONs show identical mobility with a clear band in gel electrophoresis images, indicating the integrity of drug loaded DONs. The stability of Dox-DONs was further evaluated by a drug diffusion experiment using MINI dialysis units, which was considered as a simple method to monitor and quantify the molecular diffusion from inner structures to bulk solution. The increase of Dox fluorescence in buffer suggested a slow drug release from Dox-DONs, with ≈8 and ≈12% loaded Dox diffused out from the carrier within 15 and 45 h, respectively (Figure S5b, Supporting Information). This slow diffusion kinetics indicated the high stability of Dox-DONs in buffer solution.

## 2.2. PSMA-Selective Drug Delivery by DUPA-DONs

To evaluate the cellular uptake of 6HB-DONs with and without DUPA targeting ligand, we intentionally introduced five Alexa-488 labeled ssDNA to DONs via DNA hybridization, and then compared the internalization efficiency of bare DONs and the one attached with 5 DUPA ligands by confocal imaging. After 4 h incubation, a higher Alexa-488 fluorescence signal was observed with DUPA-DONs in LNCaP cells expressing high level of PSMA<sup>[46]</sup> (Figure 2a; Figure S9, Supporting Information), indicating the positive effect of targeting ligand DUPA on selective cellular uptake of DONs. Whereas for PC-3 cells

expressing no PSMA,<sup>[44]</sup> no obvious difference of intracellular Alexa 488 fluorescence was observed, further indicating the selective targeting capability of DUPA-DONs to PSMA (Figure 2a). These confocal imaging observations were further confirmed by flow-cytometric analysis (Figure 2b).

Having established that DUPA-DONs can be selectively internalized into cells expressing PSMA, we evaluated Dox delivery by DONs and DUPA-DONs (Figure 3). Since free Dox can diffuse directly through intact cell membranes, strong Dox fluorescence were observed in cytoplasm and nucleus of LNCaP cells treated with Dox only (Figure 3, panel (i); Figure S10, Supporting Information). When Dox were loaded to DONs without DUPA ligands, only weak Dox fluorescence could be observed together with Alex-488 fluorescence (Figure 3, panel (iv); Figure S11, Supporting Information, top panel), indicating Dox could not be efficiently delivered into LNCaP cells by DONs, which is in agreement with the observation that bare DONs cannot be efficiently endocytosed by LNCaP cells (Figure 2). When Dox were loaded to DUPA-DONs, strong fluorescence of both Dox and Alex-488 were observed (Figure 3, panel (v); Figure S11, Supporting Information, bottom panel), revealing the efficient Dox delivery to LNCaP cells. In addition, DUPA-DON signals were located in cytoplasmic region and partially colocalized with lysosomes, and were not observed in nucleus, whereas Dox signals well colocalized with both DUPA-DONs and nucleus, indicating Dox were released from 6HB-DONs and then diffused into nucleus. This observation coordinates with previous study that part of Dox could be released from dsDNA in endosomes after internalized through endocytosis.<sup>[47]</sup> Therefore, the ADC-like nanocomposite, Dox-DUPA-DONs, can selectively deliver and then release Dox in PSMA positive cells in a highly efficient manner.

## 2.3. Selective Cytotoxicity of ADC-Like Nanocomposites

We then evaluated and compared cytotoxicity of free DUPA ligand, free Dox, DONs, DUPA-DONs, Dox-DONs, and

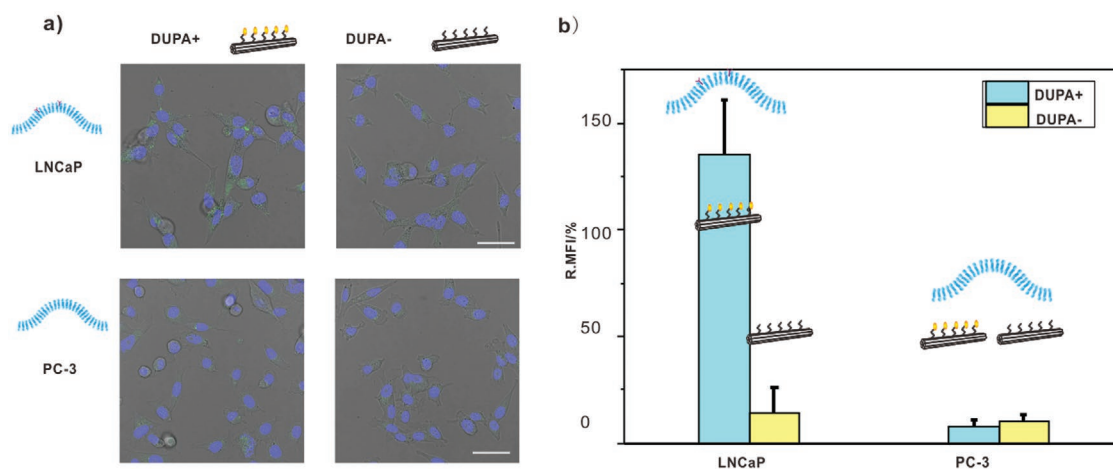


**Figure 2.** PSMA-selective cellular uptake of DUPA-DONs. a) Representative confocal images indicating the internalization of DONs (green) into target LNCaP cells with the direction of DUPA. LNCaP and PC-3 cells were both stained with Hoechst (blue). Scale bars, 50  $\mu$ m. b) Comparison of cellular uptake of DONs and DUPA-DONs by LNCaP (PSMA+) and PC-3 cells (PSMA-) revealed by flow cytometric analysis.

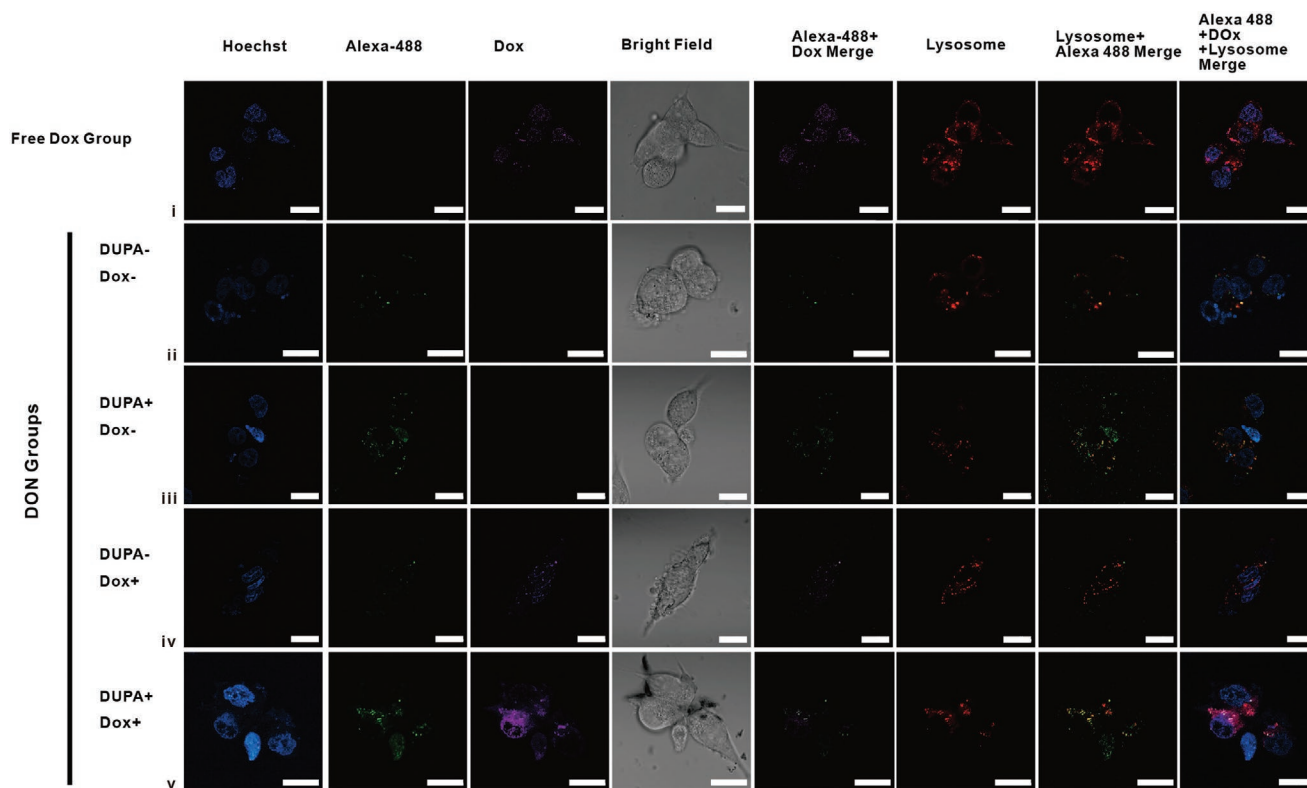


**Figure 3.** Selective drug delivery to cells revealed by confocal imaging. Dox is fluorescently emissive (magenta,  $\lambda_{\text{ex}}$  488 nm), cell nucleus are labelled with Hoechst (blue,  $\lambda_{\text{ex}}$  405 nm), DONs are labelled with Alexa-488 (green,  $\lambda_{\text{ex}}$  488 nm), lysosomes are labelled with LysoTracker (Deep Red Thermo L12492) (red,  $\lambda_{\text{ex}}$  633 nm). LNCaP cells (PSMA+) were incubated with i) free Dox ( $320 \times 10^{-9}$  M), ii) DONs ( $100 \times 10^{-12}$  M), iii) DUPA-DONs ( $100 \times 10^{-12}$  M), iv) Dox-DONs ( $100 \times 10^{-12}$  M), and v) Dox-DUPA-DONs ( $100 \times 10^{-12}$  M) for 4 h, respectively. Scale bars, 10  $\mu\text{m}$ .

Dox-DUPA-DONs against LNCaP cells and PC-3 cells (Figure 4; Figure S12, Supporting Information). The relative cell viability of LNCaP cells and PC-3 cells were monitored at 0, 3, 6, 24, and 48 h, respectively. Comparable cell viability was observed for cells treated with buffer only (negative control group), free DUPA ligand and drug-free DONs within 48 h, indicating good biocompatibility of DONs. Whereas for Dox involved treatments, a significant drop on cell viability was observed for LNCaP cells, which is contrary to PC-3 cells that only a moderate drop of cell viability was obtained with free Dox while Dox-DON showed no lethal effect. Specifically, a much stronger inhibition on LNCaP cell viability was observed for Dox-DUPA-DONs than Dox-DONs, which is also stronger than free Dox. For both LNCaP cells and PC-3 cells, free Dox group showed higher cell cytotoxicity than Dox-DON, mainly due to burst diffusion of free Dox compared to the release of Dox from DON. These results demonstrated the direction effect of DUPA on the selective cytotoxicity of Dox-DONs composite.

We also conducted another cell viability measurement through real time cell analysis (RTCA) (Figure S13, Supporting Information), by continuously monitoring the real-time electrical impedance that reflects the physiological status of cells such as cell proliferation and viability. The cell index measured before and after the addition of samples ( $t = 60$  h) demonstrated that the lethal effect of treatments is in the order of Dox-DUPA-DON > free Dox > Dox-DON > DON  $\approx$  blank control, which is in agreement of the results obtained with MTT assay.

#### 2.4. Modulation of Cytotoxicity of ADC-Like Nanocomposites via Programming Distribution of Targeting Ligands

After establishing the selective cytotoxicity of Dox-DUPA-DONs against LNCaP cells, we investigated whether the cytotoxicity could be further regulated by modulating the distribution of DUPA ligands on 6 HB-DONs. In addition to the DUPA-DONs with 5 DUPA ligands, we fabricated DUPA-DONs with 10, 20, and 30 DUPA ligands, respectively, as Dox carriers (Figure S6, Supporting Information). All of these four nanocarriers showed comparable Dox loading capacity, with 3200 Dox molecules on each DON in average. Considering the DAR of ADC is generally not more than 8, the drug-to-DON ratio (3200) is two orders of magnitude higher. By modulating the numbers of DUPA ligands, we can verify the drug-to-ligand ratio (DLR), that 5, 10, 20, and 30 DUPA ligands on one 6HB DON corresponding to a DLR of 640, 320, 160, and 106, respectively.

Real time cell index was monitored with RTCA to validate the potency of these four ADC-like nanocomposites (Figure S14, Supporting Information). Upon addition of Dox-DUPA-DON, a sudden drop on cell index occurred. After 72 h, only less than 25% of the cell index remained for all the four Dox-DUPA-DONs nanocomposites. We plotted the cell index of LNCaP cells at 48 h, with the numbers of DUPA ligands together in Figure 5, which clearly indicated the decrease of cell index along with the increase of DLR. This observation suggested a direct and strong correlation between drug potency and DLR engineering. More

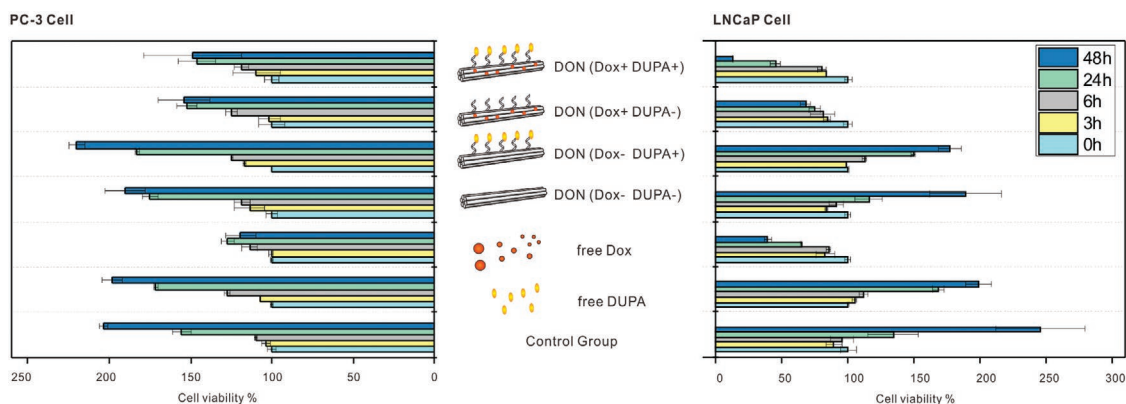


**Figure 4.** Cellular cytotoxicity analysis evaluated by MTT assay. PC-3 cells (PSMA<sup>-</sup>) and LNCaP cells (PSMA<sup>+</sup>) were treated with buffer (control group),  $1 \times 10^{-9}$  M DUPA ligand,  $320 \times 10^{-9}$  M free Dox,  $100 \times 10^{-12}$  M free DONs,  $100 \times 10^{-12}$  M DUPA-DONs,  $100 \times 10^{-12}$  M Dox-DONs and  $100 \times 10^{-12}$  M Dox-DUPA-DONs, respectively. Error bars represent the standard deviation from three independent measurements.

DUPA ligands displayed on linear six HB-DONs should increase the possibility of interactions between the ADC-like nanocomposite and PSMA<sup>+</sup> cells, which further lead to more efficient internalization of Dox-DONs and the consequent lethal effect.

### 3. Conclusions

Limited drug payload capacity and selectivity of ADC remains as a challenge to warrant pharmaceutical effect. We constructed six HB-DONs attached with targeting ligands as a new selective drug carrier platform against prostate cancer cells. Dox could be easily loaded on this platform via intercalation with dsDNA helix with a high efficiency, that 3200 Dox molecules can be loaded on each six HB-DON. We employed DUPA, a small molecule ligand targeting PSMA with high affinity, to direct selective delivery of Dox

into cells. Thus fabricated Dox-DUPA-DONs can serve as ADC-like nanocomposites, capable of targeting PASM on LNCaP cells. Accordingly, selective endocytosis and lethal effect were achieved. Compared to free Dox, Dox-DUPA-DONs showed lower toxicity against PC-3 cells (PSMA<sup>-</sup>) but much higher toxicity against LNCaP (PSMA<sup>+</sup>) cells. We further interrogated the ligand engineering by localizing different numbers of DUPA ligand on DONs and achieved increased cytotoxicity of Dox-DUPA-DONs with the increase of targeting ligands, presumably due to higher uptake efficiency originated from the enhancement of binding capability with more binding sites. These findings may provide insights for the design and optimization of DNA nanostructures as drug carrier nanoplatform for biomedical application.<sup>[48]</sup>

### Supporting Information

Supporting Information is available from the Wiley Online Library or from the author.

### Acknowledgements

Z.G., L.G., and G.W. contributed equally to this work. The authors are grateful for financial support from the National Nature Science Foundation of China (U1532119, 21775157, 31571014, and 21675167), the National Key Research and Development Program of China (2016YFA0400900 and 2016YFC1306400), and the Key Research Program of Frontier Sciences (QYZDJ-SSW-SLH031).

### Conflict of Interest

The authors declare no conflict of interest.

### Keywords

DNA nanostructures, drug carriers, drug-to-ligand ratio, framework nucleic acids, targeting ligands

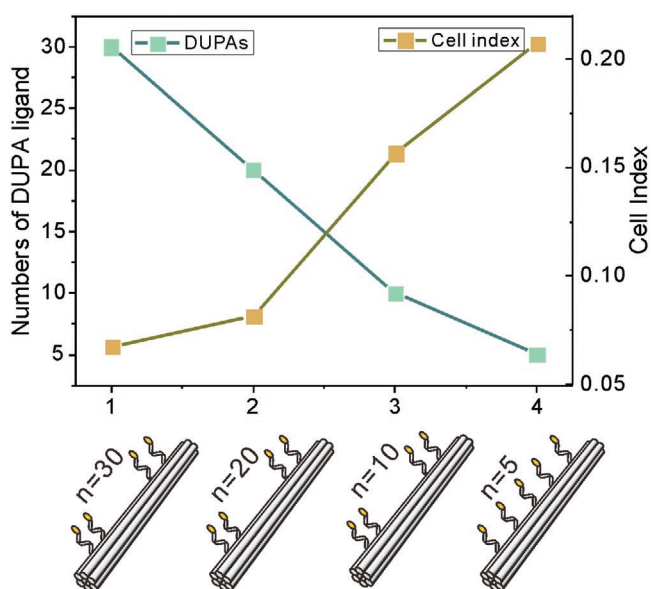


**Figure 5.** Correlation of therapeutic efficacy of Dox-DUPA-DONs with numbers of targeting ligand. Cell index of LNCaP cells (PSMA<sup>+</sup>) at 48 h was plotted with numbers of DUPA ligand (5, 10, 20, and 30) on Dox-DUPA-DONs. Concentration of Dox-DUPA-DONs,  $100 \times 10^{-12}$  M.

Received: August 27, 2019  
Revised: February 23, 2020  
Published online:

- [1] R. V. J. Chari, M. L. Miller, W. C. Widdison, *Angew. Chem., Int. Ed.* **2014**, *53*, 3796.
- [2] V. Chudasama, A. Maruani, S. Caddick, *Nat. Chem.* **2016**, *8*, 114.
- [3] R. S. Zolot, S. Basu, R. P. Million, *Nat. Rev. Drug Discovery* **2013**, *12*, 259.
- [4] E. L. Sievers, P. D. Senter, *Annu. Rev. Med.* **2013**, *64*, 15.
- [5] A. Younes, N. L. Bartlett, J. P. Leonard, D. A. Kennedy, C. M. Lynch, E. L. Sievers, A. Forero-Torres, *N. Engl. J. Med.* **2010**, *363*, 1812.
- [6] P. D. Senter, E. L. Sievers, *Nat. Biotechnol.* **2012**, *30*, 631.
- [7] S. Verma, D. Miles, L. Gianni, I. E. Krop, M. Welslau, J. Baselga, M. Pegram, D.-Y. Oh, V. Dieras, E. Guardino, L. Fang, M. W. Lu, S. Olsen, K. Blackwell, E. S. Grp, *N. Engl. J. Med.* **2012**, *367*, 1783.
- [8] P. M. LoRusso, D. Weiss, E. Guardino, S. Girish, M. X. Sliwkowski, *Clin. Cancer Res.* **2011**, *17*, 6437.
- [9] P. Ehrlich, *BMJ* **1913**, *2*, 353.
- [10] G. Badescu, P. Bryant, M. Bird, K. Henseleit, J. Swierkosz, V. Parekh, R. Tommasi, E. Pawlisz, K. Jurlewicz, M. Farys, N. Camper, X. Sheng, M. Fisher, R. Grygorash, A. Kyle, A. Abhilash, M. Frigerio, J. Edwards, A. Godwin, *Bioconjugate Chem.* **2014**, *25*, 1124.
- [11] P. M. Drake, A. E. Albers, J. Baker, S. Banas, R. M. Barfield, A. S. Bhat, G. W. de Hart, A. W. Garofalo, P. Holder, L. C. Jones, R. Kudirka, J. McFarland, W. Zmolek, D. Rabuka, *Bioconjugate Chem.* **2014**, *25*, 1331.
- [12] E. S. Zimmerman, T. H. Heibeck, A. Gill, X. Li, C. J. Murray, M. R. Madlansacay, T. Cuong, N. T. Uter, G. Yin, P. J. Rivers, A. Y. Yam, W. D. Wang, A. R. Steiner, S. U. Bajad, K. Penta, W. Yang, T. J. Hallam, C. D. Thanos, A. K. Sato, *Bioconjugate Chem.* **2014**, *25*, 351.
- [13] A. C. Stan, D. L. Radu, S. Casares, C. A. Bona, T. D. Brumeanu, *Cancer Res.* **1999**, *59*, 115.
- [14] H. Lu, Q. Zhou, V. Deshmukh, H. Phull, J. Ma, V. Tardif, R. R. Naik, C. Bouvard, Y. Zhang, S. Choi, B. R. Lawson, S. Zhu, C. H. Kim, P. G. Schultz, *Angew. Chem., Int. Ed.* **2014**, *53*, 9841.
- [15] H. Lu, D. Wang, S. Kazane, T. Javahishvili, F. Tian, F. Song, A. Sellers, B. Barnett, P. G. Schultz, *J. Am. Chem. Soc.* **2013**, *135*, 13885.
- [16] B. Q. Shen, K. Xu, L. Liu, H. Raab, S. Bhakta, M. Kenrick, K. L. Parsons-Repointe, J. Tien, S. F. Yu, E. Mai, D. Li, J. Tibbitts, J. Baudys, O. M. Saad, S. J. Scales, P. J. McDonald, P. E. Hass, C. Eigenbrot, T. Nguyen, W. A. Solis, R. N. Fuji, K. M. Flagella, D. Patel, S. D. Spencer, L. A. Khawli, A. Ebens, W. L. Wong, R. Vandlen, S. Kaur, M. X. Sliwkowski, R. H. Scheller, P. Polakis, J. R. Junutula, *Nat. Biotechnol.* **2012**, *30*, 184.
- [17] R. P. Lyon, T. D. Bovee, S. O. Doronina, P. J. Burke, J. H. Hunter, H. D. Neff-LaFord, M. Jonas, M. E. Anderson, J. R. Setter, P. D. Senter, *Nat. Biotechnol.* **2015**, *33*, 733.
- [18] K. J. Hamblett, P. D. Senter, D. F. Chace, M. M. Sun, J. Lenox, C. G. Cerveny, K. M. Kissler, S. X. Bernhardt, A. K. Kopcha, R. F. Zabinski, *Clin. Cancer Res.* **2004**, *10*, 7063.
- [19] R. A. Herbertson, N. C. Tebbutt, F. - T. Lee, D. J. MacFarlane, B. Chappell, N. Micallef, S.-T. Lee, T. Saunder, W. Hopkins, F. E. Smyth, *Clin. Cancer Res.* **2009**, *15*, 6709.
- [20] J. R. Junutula, H. Raab, S. Clark, S. Bhakta, D. D. Leipold, S. Weir, Y. Chen, M. Simpson, S. P. Tsai, M. S. Dennis, *Nat. Biotechnol.* **2008**, *26*, 925.
- [21] P. J. Carter, G. A. Lazar, *Nat. Rev. Drug Discovery* **2018**, *17*, 197.
- [22] S. Bloom, C. Liu, D. K. Kölmel, J. X. Qiao, Y. Zhang, M. A. Poss, W. R. Ewing, D. W. MacMillan, *Nat. Chem.* **2018**, *10*, 205.
- [23] F. Zhang, S. Jiang, S. Wu, Y. Li, C. Mao, Y. Liu, H. Yan, *Nat. Nanotechnol.* **2015**, *10*, 779.
- [24] N. C. Seeman, H. F. Sleiman, *Nat. Rev. Mater.* **2018**, *3*, 17068.
- [25] Q. Jiang, C. Song, J. Nangreave, X. Liu, L. Lin, D. Qiu, Z.-G. Wang, G. Zou, X. Liang, H. Yan, B. Ding, *J. Am. Chem. Soc.* **2012**, *134*, 13396.
- [26] Y.-X. Zhao, A. Shaw, X. Zeng, E. Benson, A. M. Nyström, B. Högberg, *ACS Nano* **2012**, *6*, 8684.
- [27] V. Linko, A. Ora, M. A. Kostianen, *Trends Biotechnol.* **2015**, *33*, 586.
- [28] E. Tasciotti, *Nat. Biotechnol.* **2018**, *36*, 234.
- [29] Q. Jiang, S. Liu, J. Liu, Z. G. Wang, B. Ding, *Adv. Mater.* **2018**, *31*, 1804785.
- [30] S. M. Douglas, I. Bachelet, G. M. Church, *Science* **2012**, *335*, 831.
- [31] J. Li, H. Pei, B. Zhu, L. Liang, M. Wei, Y. He, N. Chen, D. Li, Q. Huang, C. Fan, *ACS Nano* **2011**, *5*, 8783.
- [32] P. Wang, M. A. Rahman, Z. Zhao, K. Weiss, C. Zhang, Z. Chen, S. J. Hurwitz, Z. G. Chen, D. M. Shin, Y. Ke, *J. Am. Chem. Soc.* **2018**, *140*, 2478.
- [33] W. Tai, J. Li, E. Corey, X. Gao, *Nat. Biomed. Eng.* **2018**, *2*, 326.
- [34] S. P. Li, Q. Jiang, S. L. Liu, Y. L. Zhang, Y. H. Tian, C. Song, J. Wang, Y. G. Zou, G. J. Anderson, J. Y. Han, Y. Chang, Y. Liu, C. Zhang, L. Chen, G. B. Zhou, G. J. Nie, H. Yan, B. Q. Ding, Y. L. Zhao, *Nat. Biotechnol.* **2018**, *36*, 258.
- [35] A. Ora, E. Järvihaavisto, H. Zhang, H. Auvinen, H. A. Santos, M. A. Kostianen, V. Linko, *Chem. Commun.* **2016**, *52*, 14161.
- [36] Q. Mei, X. Wei, F. Su, Y. Liu, C. Youngbull, R. Johnson, S. Lindsay, H. Yan, D. Meldrum, *Nano Lett.* **2011**, *11*, 1477.
- [37] D. Jiang, Z. Ge, H.-J. Im, C. G. England, D. Ni, J. Hou, L. Zhang, C. J. Kutyreff, Y. Yan, Y. Liu, S. Y. Cho, J. W. Engle, J. Shi, P. Huang, C. Fan, H. Yan, W. Cai, *Nat. Biomed. Eng.* **2018**, *2*, 865.
- [38] H. Ding, J. Li, N. Chen, X. Hu, X. Yang, L. Guo, Q. Li, X. Zuo, L. Wang, Y. Ma, C. Fan, *ACS Cent. Sci.* **2018**, *4*, 1344.
- [39] Z. Ge, H. Gu, Q. Li, C. Fan, *J. Am. Chem. Soc.* **2018**, *140*, 17808.
- [40] Z. Y. He, W. L. Zhang, S. F. Mao, N. Li, H. F. Li, J. M. Lin, *Anal. Chem.* **2018**, *90*, 5540.
- [41] C. H. Kim, J. Y. Axup, B. R. Lawson, H. Yun, V. Tardif, S. H. Choi, Q. Zhou, A. Dubrovskaya, S. L. Biroc, R. Marsden, J. Pinstaff, V. V. Smider, P. G. Schultz, *Proc. Natl. Acad. Sci. USA* **2013**, *110*, 17796.
- [42] L. He, D. Lu, H. Liang, S. Xie, X. Zhang, Q. Liu, Q. Yuan, W. Tan, *J. Am. Chem. Soc.* **2018**, *140*, 258.
- [43] Y. Geng, P. Dalhaimer, S. Cai, R. Tsai, M. Tewari, T. Minko, D. E. Discher, *Nat. Nanotechnol.* **2007**, *2*, 249.
- [44] L. A. Stearns, R. Chhabra, J. Sharma, Y. Liu, W. T. Petuskey, H. Yan, J. C. Chaput, *Angew. Chem., Int. Ed.* **2009**, *48*, 8494.
- [45] P. W. K. Rothmund, *Nature* **2006**, *440*, 297.
- [46] M. D. Henry, S. H. Wen, M. D. Silva, S. Chandra, M. Milton, P. J. Worland, *Cancer Res.* **2004**, *64*, 7995.
- [47] G. Zhu, J. Zheng, E. Song, M. Donovan, K. Zhang, C. Liu, W. Tan, *Proc. Natl. Acad. Sci. USA* **2013**, *110*, 7998.
- [48] S. Surana, A. R. Shenoy, Y. Krishnan, *Nat. Nanotechnol.* **2015**, *10*, 741.